JOURNAL OF MAGNETIC RESONANCE 99, 118–138 (1992)

The Inverse Scattering Transform and Its Use in the Exact Inversion of the Bloch Equation for Noninteracting Spins

DAVID E. ROURKE AND PETER G. MORRIS

Magnetic Resonance Centre, Department of Physics, University of Nottingham, Nottingham, NG7 2RD, England

Received July 16, 1991; revised December 5, 1991

A general analytic inversion of the undamped Bloch equation to produce frequency-selective pulses is described. It is shown how the results of inverse scattering theory can be applied in order to determine the possibly complex pulse that will produce any desired magnetization response. The theory is directed principally at the problem of determining phase-compensated selective pulses. The easier problem of determining selective pulses that require subsequent refocusing is also discussed. Symmetry properties of the system are examined and a powerful result—that a symmetric magnetization response can *only* be achieved with a real pulse—is proved. The inversion is used to determine phase-compensated selective 90° and doubly selective 90° pulses. It is shown that the pulses can be designed to make the responses as close to perfect as is required. An arbitrarily good selective 90° pulse that requires subsequent refocusing is also obtained, and its relationship with the equivalent pulse obtained via Fourier analysis is discussed. The sensitivity to B_1 inhomogeneity is considered—the pulses that need subsequent refocusing are found to be less sensitive than the self-refocused equivalents.

Frequency-selective pulses were first proposed by Garroway, Grannell, and Mansfield (*1*). They play a central role in the majority of magnetic resonance imaging experiments, where they are used in conjunction with an applied linear magnetic field gradient to isolate a slice of controlled thickness and orientation from within an extended object. Selective pulses feature too in many of the more successful magnetic resonance spectroscopy (MRS) methods. Although at present little exploited, they hold great promise for conventional high-resolution spectroscopy. Potential applications include solvent suppression without distortion of the frequency response, magnetization transfer, and reduction of bandwidth in two- and three-dimensional high-resolution experiments.

The guiding principle for the design of selective pulses has been Fourier-transform theory (*2*). Unfortunately, the NMR spin system is nonlinear and this approach gives acceptable results only in the case of small flip angles, for which the system is approximately linear. The inappropriateness of Fourier-transform theory is manifest in the departure from perfectly square excitation profiles and the presence of unwanted side lobes.

A further problem, common to both MRI and MRS, is the dephasing of the xy magnetization that generally occurs during simple selective pulses. For most pulses, the phase shift is approximately first order and corresponds to evolution at the relevant offset for half the pulse length (*2*). If the RF pulses are spatially selective (i.e., applied

0022-2364/92 $5.00

in the presence of a magnetic field gradient), the transverse magnetization can be refocused using a negative gradient lobe, whose area is one-half that of the positive lobe applied during the RF pulse. Refocusing is time consuming because it requires the gradients to be ramped down, ramped up in the negative direction, left on for a time approaching half the pulse length, and then ramped down to zero again. Gradients cannot be switched too fast because of the rise times associated with the inductance of the gradient coils themselves, the rise times of the gradient drivers, and the effects of eddy currents in the magnet bore if properly shielded gradient sets are not employed. A similar problem exists for high-resolution applications where the phase accumulation appears as a first-order shift across the spectrum. Although no gradients are involved, refocusing is necessary and must be achieved using a π pulse. A delay corresponding to at least half the width of the selective pulse is incurred, which could prove disastrous in the case of short T_2 species. Recently, several optimization schemes including simulated annealing (*3–6*), SPINCALC (*7, 8*), and natural selection (*9*) have enjoyed some success in the generation of novel pulses, including some which are inherently phase compensated.

The ideal method of selective-pulse design analytically generates the exact pulse required to achieve any specified excitation profile. Unfortunately, specific inverse solutions of the Bloch equation are rare. The classic example is the complex hyperbolic secant pulse (*10, 11*), which gives almost perfect inversion over a slice. Unfortunately, it is not a refocusing ("pancake flip") pulse and so does not solve the problem of providing a good π pulse for multislice spin-echo imaging experiments. However, its use has been crucial to the success achieved by the ISIS method of spatial selection.

We introduce here a new analytic method based on the inverse scattering transform (IST). The IST has been found to be a particularly powerful tool in mathematics and physics. It was first developed by Gel'fand and Levitan (*12*), Marchenko (*13*), and Kay and Moses (*14*) to determine the potential required to obtain given scattering coefficients of a wavefunction in one dimension. The theory was greatly extended by Gardner *et al.* (*15*), Zakharov and Shabat (*16*), and Ablowitz *et al.* (*17*), who realized that the IST could be used as the nonlinear generalization of the Fourier transform in solving a class of nonlinear differential equations.

In a rather complex sequence of transformations, Lamb (*18*) showed how to use the IST to obtain a lossless real pulse in coherent optics, where the system obeys the coupled Maxwell–Bloch equations. We shall describe a method of obtaining an arbitrary response profile as a function of frequency offset for a system obeying the undamped Bloch equation, with the resultant pulse envelope allowed real or complex.

THEORY

The Bloch equation with no relaxation is conventionally written

$$\frac{\partial \mathbf{m}}{\partial t} = \gamma \mathbf{m} \times \mathbf{B}, \qquad [1]$$

where $\mathbf{m}(\nu, t)$ is the magnetization vector and is a function of frequency offset ν and time t, γ is the gyromagnetic ratio, and $\mathbf{B}(\nu, t)$ is the magnetic field $=[B_1(t), B_2(t), B_3(\nu)]$.

This equation simply states that the magnetization vector rotates about vector $\gamma\mathbf{B}$ with angular velocity $-\gamma|\mathbf{B}|$. It can be shown (see, e.g., (*19*)) that Eq. [1] can be rewritten as

$$\frac{\partial\psi}{\partial t} = -\frac{1}{2}\, i\omega\cdot\sigma\psi, \qquad [2]$$

where ψ is the spinor associated with the magnetization $\mathbf{m}(\nu, t)$. It describes the total rotation experienced by that magnetization. The vector $\omega = [\omega_1(t), \omega_2(t), \nu] = -\gamma\mathbf{B}$ is the instantaneous angular velocity at time t, resonance offset ν, and $\sigma = (\sigma_1, \sigma_2, \sigma_3)$ are the Pauli matrices

$$\sigma_1 = \begin{bmatrix} 0 & 1 \\ 1 & 0 \end{bmatrix}, \qquad \sigma_2 = \begin{bmatrix} 0 & -i \\ i & 0 \end{bmatrix}, \qquad \text{and} \qquad \sigma_3 = \begin{bmatrix} 1 & 0 \\ 0 & -1 \end{bmatrix}. \qquad [3]$$

If we now define $\xi = \frac{1}{2}\nu T$, $q = -\frac{1}{2}i\omega^* T$, and $\tau = t/T$, where $\omega = \omega_1 + i\omega_2$,* denotes the complex conjugate, and T is some arbitrary scale factor with the dimension time, we can write Eq. [2] as the dimensionless equation

$$\frac{\partial\psi(\xi, \tau)}{\partial\tau} = \begin{bmatrix} -i\xi & q(\tau) \\ -q^*(\tau) & i\xi \end{bmatrix}\psi(\xi, \tau), \qquad [4]$$

which is in the form usually associated with the IST.

When applied to inverse scattering, $q(\tau)$ represents a potential which scatters the incident quantum-mechanical wavefunction ψ to produce transmitted and reflected wavefunctions. The amplitudes of the incident, transmitted, and reflected wavefunctions are related by the *scattering matrix*. Inverse scattering theory is used to determine the form of the potential given this scattering matrix.

When applied to the inversion of the Bloch equation, $q(\tau)$ describes the pulse envelope, as shown above. The scattering matrix will be found to be simply related to the final magnetization profile. Hence we find that the IST enables us to determine the pulse required to give any desired magnetization profile. We shall derive the principal results of the inverse scattering transform and then apply these results in order to invert the Bloch equation. More complete details on the derivation of the IST can be found in (*17*).

DERIVATION OF THE IST

Equation [4] is a second-order equation and hence has two linearly independent solutions. Assuming $q(\tau) \to 0$ as $\tau \to \pm\infty$, we can let two such solutions be ψ_+ and $\hat{\psi}_+$, where

$$\psi_+(\tau, \xi) \to \begin{bmatrix} e^{-i\xi\tau} \\ 0 \end{bmatrix} \qquad \text{and} \qquad \hat{\psi}_+(\tau, \xi) \to \begin{bmatrix} 0 \\ e^{i\xi\tau} \end{bmatrix} \qquad \text{as } \tau \to \infty. \qquad [5]$$

Let another two solutions be ψ_- and $\hat{\psi}_-$, which will be linearly dependent on ψ_+ and $\hat{\psi}_+$,

$$\psi_-(\tau, \xi) \to \begin{bmatrix} e^{-i\xi\tau} \\ 0 \end{bmatrix} \qquad \text{and} \qquad \hat{\psi}_-(\tau, \xi) \to \begin{bmatrix} 0 \\ -e^{i\xi\tau} \end{bmatrix} \qquad \text{as } \tau \to -\infty. \qquad [6]$$

These solutions are linearly related by the scattering matrix, so if Ψ_- is a matrix with columns ψ_- and $\hat{\psi}_-$ [which we denote as $\Psi_- = \text{mat}(\psi_-, \hat{\psi}_-)$] and similarly $\Psi_+ = \text{mat}(\psi_+, \hat{\psi}_+)$, then

$$\Psi_- = \Psi_+ \mathbf{S}, \tag{7}$$

where $\mathbf{S}$ is a matrix:

$$\mathbf{S} = \begin{bmatrix} a(\xi) & \hat{b}(\xi) \\ b(\xi) & -\hat{a}(\xi) \end{bmatrix}. \tag{8}$$

Inverse scattering theory applied to Eq. [4] shows us that if we define

$$f(\tau) = \frac{1}{2\pi} \int_{C_+} \frac{b(\xi)}{a(\xi)} e^{i\xi\tau} d\xi, \tag{9}$$

where the integration is over a contour from $-\infty$ to $+\infty$ in the upper-half complex plane over all poles of b/a, then

$$q(\tau) = -2K_{12}(\tau, \tau), \tag{10}$$

where

$$\mathbf{K}(\tau, \tau') + \mathbf{F}(\tau + \tau') + \int_\tau^\infty \mathbf{K}(\tau, \tau'')\mathbf{F}(\tau' + \tau'')d\tau'' = 0 \tag{11}$$

and

$$\mathbf{K} = \begin{bmatrix} K_{11} & K_{12} \\ -K_{12}^* & K_{11}^* \end{bmatrix}, \qquad \mathbf{F} = \begin{bmatrix} 0 & -f^* \\ f & 0 \end{bmatrix}. \tag{12}$$

Hence we can recover $q(\tau)$ from the reflection coefficient $r(\xi) = b/a$ by solving Eq. [11], the matrix Marchenko equation. Before doing that, we obtain the relationship between $r(\xi)$ and the desired magnetization profile.

THE REFLECTION COEFFICIENT AND THE FINAL MAGNETIZATION

First we note that as $\tau \to -\infty$, the spinor $\psi(\tau, \nu)$ must tend to $\begin{bmatrix} e^{-i\xi\tau} \\ 0 \end{bmatrix}$ since this corresponds to rotation about the z axis, the equilibrium orientation, and hence to an apparently unperturbed magnetization.

Hence $\psi = \psi_-(\tau, \xi)$ is the solution to [4], so the asymptotic form as $\tau \to +\infty$ is, from Eqs. [5]–[8],

$$\psi \to \begin{bmatrix} ae^{-i\xi\tau} \\ be^{i\xi\tau} \end{bmatrix} \qquad \text{as } \tau \to \infty. \tag{13}$$

Now, standard spinor theory [e.g., see (*20*)] shows that a vector initially at (0, 0, 1), when rotated by the spinor in Eq. [13], becomes (m_1, m_2, m_3), where

$$m = m_1 + im_2 = 2a^*be^{2i\xi\tau} \qquad \text{as } \tau \to \infty$$

$$m_3 = |a|^2 - |b|^2. \tag{14}$$

Hence, using the identity shown in Ref. (*17*) that $|a|^2 + |b|^2 = 1$ for real ξ, we can show that

$$r(\xi) = \frac{m(\xi)e^{-2i\xi\tau}}{1 + m_3(\xi)} \qquad \text{as } \tau \to \infty \qquad [15]$$

and we note that there is in fact no dependence on τ on the right-hand side of Eq. [15], as $m(\xi) \sim e^{2i\xi\tau}$ as $\tau \to +\infty$.

We also note that Ablowitz *et al.* in Ref. (*17*) show that in the limit of $r(\xi) \to 0$, $q(\tau)$ is given simply by the Fourier transform of the reflection coefficient, and hence to the Fourier transform of the "unwound" magnetization $m(\xi)e^{-2i\xi\tau}$, and so we see that this theory is indeed a nonlinear generalization of the simple Fourier treatment often used in pulse design.

SOLUTION OF THE MARCHENKO EQUATION

Recall that we need to solve Eq. [11], the matrix Marchenko equation. In Ref. (*17*), existence and uniqueness of a solution to [11] for the system [4] are shown. To actually obtain the solution, we use a method analogous to that described by Moses and Prosser (*21*). We describe $r(\xi)$ as a rational polynomial,

$$r(\xi) = \frac{\alpha \prod_{j=1}^{m} (\xi - z_j)}{\prod_{k=1}^{n} (\xi - p_k)}, \qquad [16]$$

where α is a constant, z_j are the zeroes of $r(\xi)$, and p_k are the poles of $r(\xi)$ (all defined in the complex plane). This describes all functions with a finite number of zeroes and poles. Other "irrational" functions are considered by approximating $r(\xi)$ by a rational function and then letting m or n tend to infinity. Note that we require $n > m$ if $r(\xi) \to 0$ as $|\xi| \to \infty$ (which we want to be the case).

It is then possible to show that, given this form for $r(\xi)$, the function $q(\tau)$ must have the form

$$q(\tau) = \begin{cases} -2 \sum_{j=1}^{2n} M_j(\tau)e^{-i\phi_j\tau} & \text{for } \tau < 0 \\ 0 & \text{for } \tau > 0, \end{cases} \qquad [17]$$

where the ϕ_j are the $2n$ solutions of the polynomial equation

$$r(\xi)r^*(\xi^*) = -1 \qquad [18]$$

noting that if ϕ_j is a solution of Eq. [18], then so is ϕ_j^*.

The M_j are the $2n$ solutions of the linear matrix equation

$$\begin{aligned} &\sum_{j=1}^{2n} \frac{e^{-i\phi_j\tau}}{\phi_j - p_k} M_j(\tau) = 0 \\ &\qquad\qquad \text{for } k = 1 \cdots n. \\ &i \sum_{j=1}^{2n} \frac{e^{i\phi_j\tau}}{\phi_j - p_k^*} r(\phi_j)M_j(\tau) = 1 \end{aligned} \qquad [19]$$

We then obtain the complex pulse profile from

$$w(t) = -2iq^*(t/T)/T. \qquad [20]$$

ALTERNATIVE SOLUTION

There are several possible methods for attempting to solve the Marchenko equation [11]. We have described the method of using a rational polynomial because it automatically ensures that the pulse is zero after $\tau = 0$, which we shall find makes it easy to design self-refocused pulses.

For pulses that need refocusing by, for example, a gradient reversal or a 180° hard pulse, we find that these are most conveniently calculated by an iterative method. We define

$$\mathbf{K}_0(\tau, \tau') = -\mathbf{F}(\tau + \tau'), \qquad [21]$$

where $\mathbf{F}(\tau)$ is as defined in Eq. [12], and hence $\mathbf{K}_0$ is a matrix. Furthermore, we define

$$\mathbf{K}_{j+1}(\tau, \tau') = -\mathbf{F}(\tau + \tau') - \int_{\tau}^{\infty} \mathbf{K}_j(\tau, \tau'')\mathbf{F}(\tau' + \tau'')d\tau''. \qquad [22]$$

By consideration of [11] we see that if $\mathbf{K}_j$ tends to a limiting form as $j \rightarrow \infty$, say $\mathbf{K}_j \rightarrow \mathbf{K}$, then $\mathbf{K}(\tau, \tau')$ satisfies Eq. [11].

Now consider Eq. [9],

$$f(\tau) = \frac{1}{2\pi} \int_{C_+} r(\xi) e^{i\xi\tau} d\xi,$$

where $r(\xi) = b(\xi)/a(\xi)$. Using complex analysis we can write this as

$$f(\tau) = \frac{1}{2\pi} \int_{-\infty}^{\infty} r(k) e^{ik\tau} dk - i \sum_{n=1}^{N} c_n e^{i\xi_n \tau}, \qquad [23]$$

where ξ_n are the N poles of $r(\xi)$ in the upper half-plane, with c_n the corresponding residues. If $r(\xi)$ has poles in the upper half-plane, $f(\tau)$ will blow up as τ tends to $-\infty$, suggesting that the iterative procedure [22] will not converge. Hence we shall use Eqs. [21] and [22] only for reflection coefficients that have no poles in the upper half-plane. Such a system is said to have no discrete spectrum. We shall see that this gives rise to an important class of pulses—pulses closely related to those obtained via simple Fourier transformation of the required magnetization profile. This might be expected, as the function $\mathbf{K}_0(\tau, \tau')$ is defined in terms of the Fourier transform of the reflection coefficient.

SYMMETRIES

It is helpful to consider simplifications that can be made when certain symmetry conditions are met. The most common condition is that

$$r(\xi) = -r^*(-\xi^*). \qquad [24]$$

Equation [15] together with the requirement that $r(\xi)$ be an analytic function of ξ shows that [24] is equivalent to the conditions that for real ξ

$$\begin{aligned} m_1(\xi) &= -m_1(-\xi) \\ m_2(\xi) &= m_2(-\xi) \\ m_3(\xi) &= m_3(-\xi). \end{aligned} \qquad [25]$$

A well-known result is that a real pulse will lead to this symmetry in the response (*22*).

However, a more powerful result is that, to get the symmetry [25], we *must* have a real pulse. We can prove this by consideration of Eqs. [9]–[12] (and hence we do not need to assume that the reflection coefficient is a rational function). From [9] we have

$$f(\tau) = \frac{1}{2\pi} \int_{C_+} r(\xi) e^{i\xi\tau} d\xi.$$

We can show that if $r(\xi) = -r^*(-\xi^*)$, then

$$f(\tau) = -f^*(\tau). \qquad [26]$$

By consideration of Eqs. [11] and [12] we can decouple K_{11} and K_{12}, and we can show that K_{12} must obey the equation

$$K_{12}(\tau, \tau') - f^*(\tau + \tau') + \int_\tau^\infty \int_\tau^\infty K_{12}(\tau, \tau''') f(\tau'' + \tau''') f^*(\tau' + \tau'') d\tau''' d\tau'' = 0. \qquad [27]$$

We can now use [26] to show that if $K_{12}(\tau, \tau')$ is a solution of [27], then so is $-K_{12}^*$. But we have already observed that the Marchenko equation [11] has a unique solution. Therefore we conclude that

$$K_{12}(\tau, \tau') = -K_{12}^*(\tau, \tau') \qquad [28]$$

and so $K_{12}(\tau, \tau')$ is purely imaginary. We therefore conclude (Eqs. [10] and [20]) that $q(\tau)$ is purely imaginary and $\omega(t)$ is purely real. This is an important theoretical result. We also find that we can reduce the orders of Eqs. [18] and [19] given the symmetry [24].

An additional symmetry often found is

$$r(\xi) = r(-\xi), \qquad [29]$$

which, together with [24], expresses the requirement that m_1 be zero over all real ξ. This corresponds to requiring that the response be phase compensated. Equations [24] and [29] reduce [18] to the equation

$$r(\phi_j) = +1 \qquad [30]$$

with each root ϕ_j having three other associated roots: $-\phi_j$, $-\phi_j^*$, and ϕ_j^*.

EXAMPLE 1

Consider the reflection coefficient

$$r(\xi) = \frac{\alpha}{\xi - i\beta}, \qquad [31]$$

where β is real and α is complex. This is the simplest nontrivial reflection coefficient. From eq. [15], the magnetization profiles are obtained from the reflection coefficient as

$$me^{-2i\xi\tau} = \frac{2r}{1 + |r|^2}$$

$$m_3 = \frac{1 - |r|^2}{1 + |r|^2} \qquad [32]$$

and hence, for $\alpha = \beta = 2$ and $T = 10^{-3}$ s, the single-pole function [31] has corresponding magnetization profiles at $\tau = 0$ as shown in Fig. 1. We have set $\alpha = \beta$, so the pulse gives a 90° rotation at resonance ($\xi = 0$).

Straightforward application of Eqs. [17]–[20] gives the pulse envelope

$$\omega(t) = \begin{cases} \dfrac{4\alpha\gamma/T}{\beta \sinh 2\gamma t/T + \gamma \cosh 2\gamma t/T} & \text{for } \tau < 0 \\ 0 & \text{for } \tau > 0, \end{cases} \qquad [33]$$

where $\gamma = \sqrt{\alpha\alpha^* + \beta^2}$. This is shown in Fig. 2.

This pulse is, in fact, quite similar to a half-Gaussian pulse (as are the magnetization responses), perhaps explaining why half-Gaussians work as well as they do (*23*). As expected from the symmetry results, the pulse is real if α is real, as then $r(\xi) = -r^*(-\xi^*)$. We did not insist that $r(\xi) = r(-\xi)$ (i.e., that $m_1 = 0$), and hence we had to solve the full polynomial equation [18].

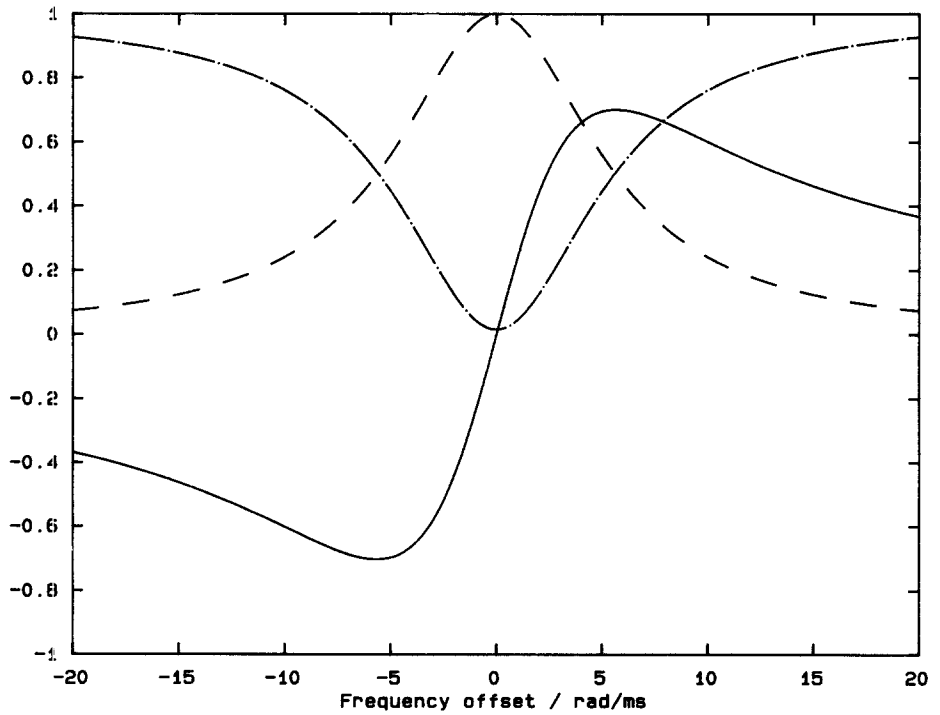

FIG. 1. The magnetization profiles corresponding to a reflection coefficient with one pole. In all figures, m_x is plotted with a solid line, m_y with a dashed line, and m_z with a dot-dashed line.

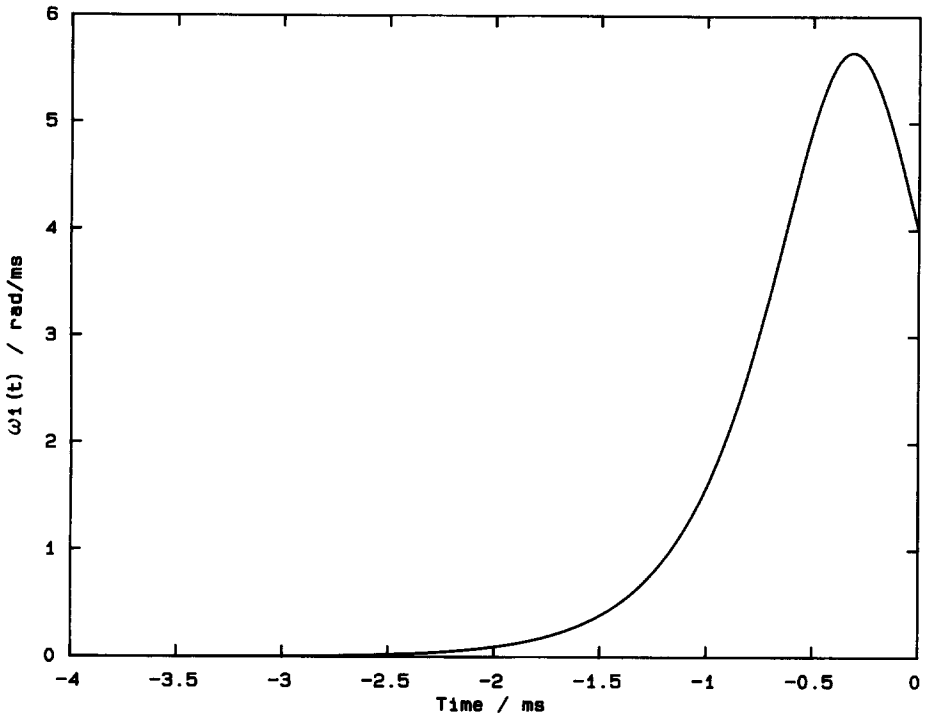

FIG. 2. The pulse envelope that gives rise to a single-pole reflection coefficient.

EXAMPLE 2

Although Eqs. [18] and [19] can be solved analytically for $n \leqslant 2$ and for special choices of $r(\xi)$, in general it is only practicable to solve them numerically. To illustrate such a solution, we will obtain the pulse profile for a 90° selective pulse, by determining the reflection coefficient for the problem, approximating this by a rational function, and evaluating the pulse profile from this approximation. By consideration of the pulse profile as we make the approximation more accurate, we can (at least qualitatively) determine the limiting form of the pulse.

An ideal 90° selective pulse will have the final magnetization profile (defined for ξ real)

$$\begin{aligned} m_1 &= 0 \qquad \text{for all } \xi \\ m_2 &= \begin{cases} 0 & \text{for } |\xi| > L/2 \\ 1 & \text{for } |\xi| \leqslant L/2 \end{cases} \\ m_3 &= \begin{cases} 1 & \text{for } |\xi| > L/2 \\ 0 & \text{for } |\xi| \leqslant L/2, \end{cases} \end{aligned} \tag{34}$$

where $L/2$ is the half-width of the excitation.

From eq. [17], the pulse obtained by this method will be zero for $\tau > 0$, so we choose time $\tau = 0$ to be the point at which we want the magnetization to be as in [34]. Then the reflection coefficient of an ideal 90° selective pulse is given by

$$r(\xi) = \begin{cases} 0 & \text{for } |\xi| > L/2 \\ i & \text{for } |\xi| \leq L/2 \end{cases} \qquad \text{with } \xi \text{ real.} \qquad [35]$$

Such a function can be approximated arbitrarily closely by the analytic function

$$r_\mu(\xi) = (1/4)ie^{\mu L}\operatorname{sech} \mu(\xi + L/2)\operatorname{sech} \mu(\xi - L/2) \qquad [36]$$

with $r_\mu(\xi) \to r(\xi)$ as $\mu \to \infty$ (μ determines the sharpness of the slice's transition region). Furthermore, by consideration of the poles and zeroes of the function [36], we can easily see that $r_\mu(\xi)$ can itself be approximated by the rational polynomial

$$r_{\mu,n}(\xi) = \frac{i}{\prod_{j=1}^{n}(1 - \xi/p_j)}, \qquad [37]$$

where, for $j = 1 \cdots n/4$,

$$\begin{aligned} p_j &= L/2 + i(j - 1/2)\pi/\mu \\ p_{j+n/4} &= p_j^* \\ p_{j+n/2} &= -p_j^* \\ p_{j+3n/4} &= -p_j \end{aligned} \qquad [38]$$

As $\mu \to \infty$ and $n \to \infty$, $r_{\mu,n} \to r(\xi)$ defined in Eq. [35].

We now solve Eqs. [18] and [19] for the rational function [37]. By using standard numerical techniques together with help from the symmetries [24] and [29] we have solved the system for $n = 20$ and $n = 84$.

The algorithm is fast. For example, for $n = 20$ and with the pulse evaluated at 1000 points, it took under 20 cpu seconds on a RISC workstation. The results are shown in Figs. 3 and 4. In both, μ was set to 2, L to 5, and T to 10^{-3} s. We have subsequently simulated each pulse via numerical integration of the Bloch equation. The resultant magnetization responses are shown together with the pulses. These agree with the predicted responses, confirming that the IST algorithm is valid.

These responses have negligible phase errors and are extremely clean over the whole frequency range (not just the range shown in the graphs). The only significant deviation from an ideal 90° pulse is in the m_3 response inside the slice. This can be improved by as much as required simply by increasing the number of poles in [37].

As might be expected, the $n = 84$ pulse has a much larger amplitude and more rapid oscillations than the $n = 20$ pulse. An unexpected feature is that it dies away before $t = 0$ (although it is not compelled to do so), making it similar in functionality to the prefocused pulses of, e.g., (*8*), obtained by numerical optimization.

EXAMPLE 3

We now illustrate how a doubly selective 90° pulse can be obtained. Such a pulse would be of interest in spectroscopy if two resonances are to be examined, and the rest of the spectrum is to be suppressed. Alternatively, we could use such a pulse to selectively suppress two peaks by selectively exciting them and applying a spoiler gradient.

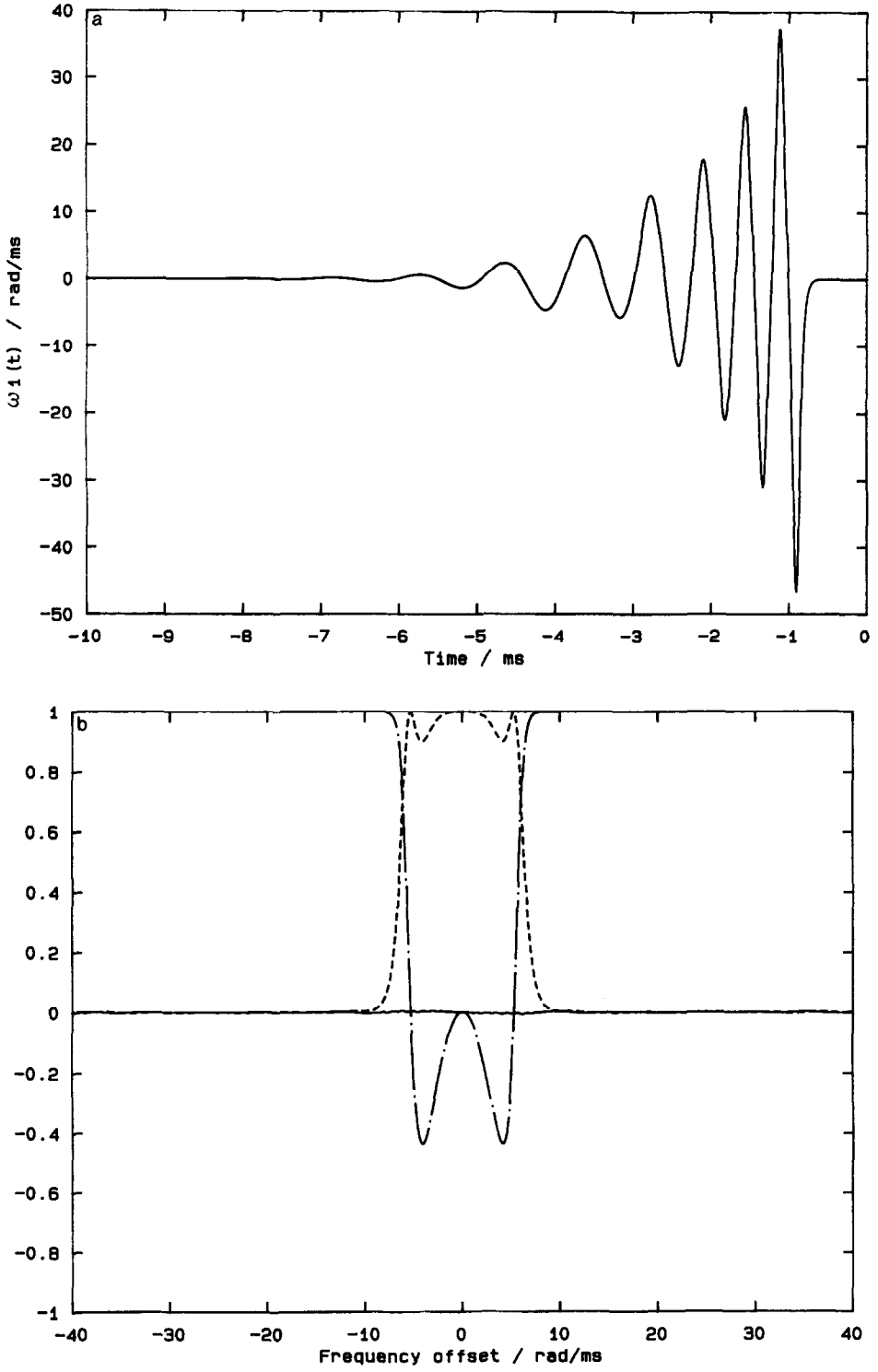

FIG. 3. (a) The pulse envelope and (b) the response to this pulse, obtained from the IST of a 20-pole rational approximation to a 90° selective pulse.

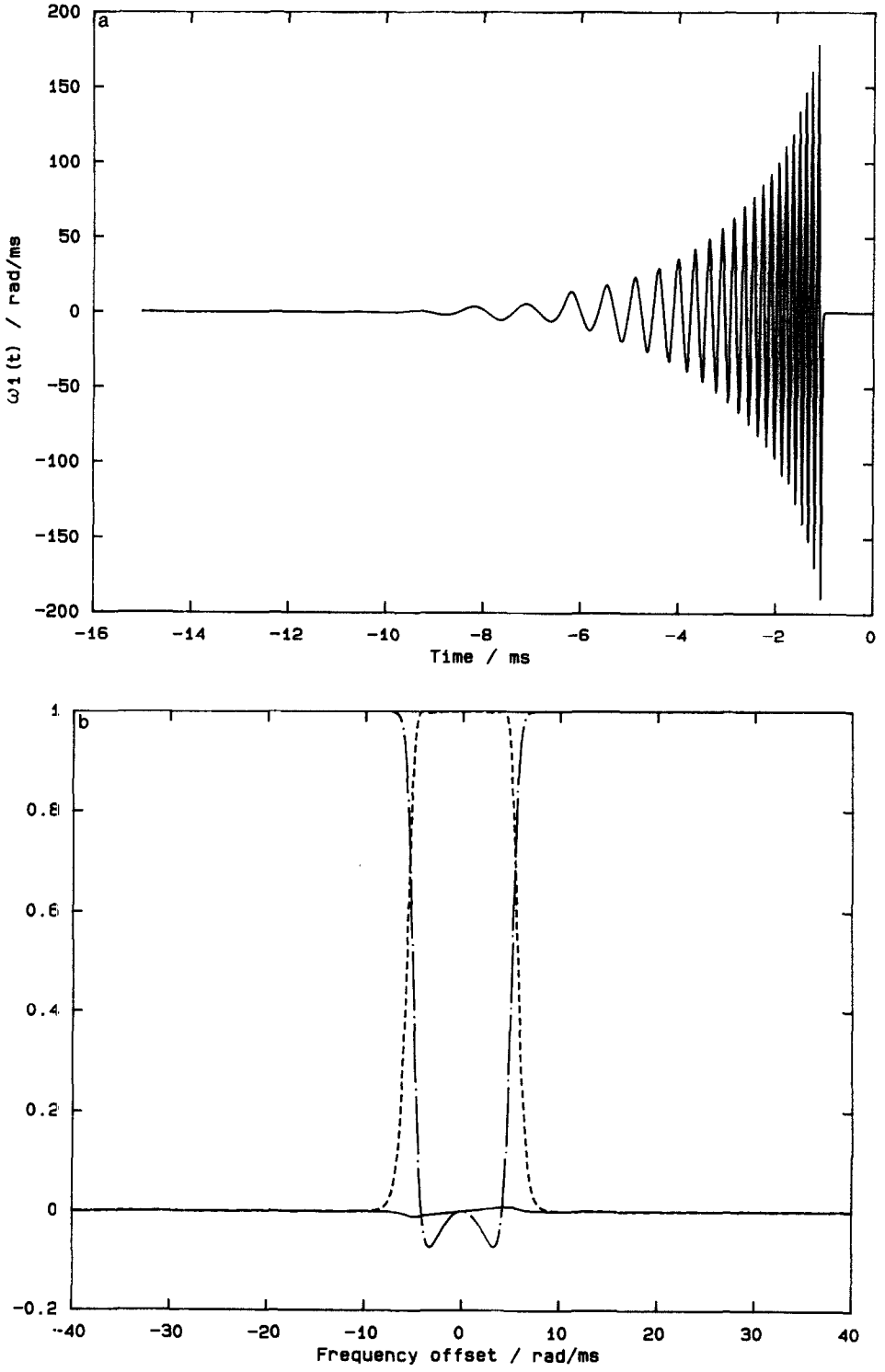

FIG. 4. (a) The pulse envelope and (b) the response to this pulse, obtained from the IST of an 84-pole rational approximation to a 90° selective pulse.

Repeating the steps taken in the previous example, we note that the function

$$r_\mu(\xi) = \frac{1}{4} ie^{\mu L}\left[\operatorname{sech} \mu\left(\xi - \frac{M+L}{2}\right)\operatorname{sech} \mu\left(\xi - \frac{M-L}{2}\right)\right.$$
$$\left. + \operatorname{sech} \mu\left(\xi + \frac{M-L}{2}\right)\operatorname{sech} \mu\left(\xi + \frac{M+L}{2}\right)\right] \quad [39]$$

gives an arbitrarily good approximation to the reflection coefficient for 90° excitation at $\xi = \pm M/2$, with each slice of width L.

By consideration of the poles and zeroes of [39], we see that the rational function

$$r_{\mu,n}(\xi) = \frac{\alpha \prod_{j=0}^{n} (1 - \xi/z_j)(1 + \xi/z_j)}{\prod_{j=0}^{2n+1} (1 - \xi/p_j)(1 - \xi/p_j^*)(1 + \xi/p_j)(1 + \xi/p_j^*)}, \quad [40]$$

where α is chosen so that $r_{\mu,n}(\pm M/2) = i$, is an arbitrarily good approximation to the required reflection coefficient. Here, $z_j = i(j + \frac{1}{2})\pi/(2\mu)$, $p_{2j} = (M - L)/2 + i(j + \frac{1}{2})\pi/\mu$, and $p_{2j+1} = (M + L)/2 + i(j + \frac{1}{2})\pi/\mu$. We note that both the symmetries [24] and [29] are present.

We used our IST algorithm to invert this system, for $n = 3$ and $n = 7$. In each, we set $M = 10$, $L = 2$, and $\mu = 4$. Given the pulse profiles, we numerically determined the magnetization responses. The pulse profile for $n = 7$ is shown in Fig. 5, with the corresponding magnetization responses. As in the previous example, the responses are very close to ideal (again, this is over the whole frequency range). Any nonideal behavior in the response would be improved by increasing n and μ.

The $n = 3$ pulse profile (evaluated at 1000 points) was obtained in less than 1 cpu minute on our workstation, suggesting that it would be feasable to implement the IST algorithm in a spectrometer, rapidly producing tailor-made pulses.

COMPARISON WITH PULSE OBTAINED VIA FOURIER ANALYSIS

It is interesting to compare the pulses obtained in example 3 with pulses that would be obtained using standard Fourier analysis. Such analysis would lead us to use a sinc pulse, with a cosine modulation. This would be followed by a hard 180° pulse and then a period of free precession for a time $T/2$, where T is the length of the original pulse.

More precisely, we choose a pulse envelope

$$\omega(t) = \begin{cases} 2A \operatorname{sinc}(\nu_0 t)\cos(\nu_1 t) & \text{for } -T/2 \leq t < T/2 \\ 0 & \text{for } T/2 \leq t < T, \end{cases} \quad [41]$$

where ν_0 is the half-width of each selected slice and ν_1 is the offset of each slice from resonance. A is a scaling factor and is such that

$$A \int_{-T/2}^{T/2} \operatorname{sinc}(\nu_0 t)dt = \pi/2, \quad [42]$$

ensuring that the pulse gives 90° excitation in each slice. A consequence of the slices being away from resonance is that we must make

$$\nu_1 T = 2n\pi, \qquad \text{where } n \text{ is an integer.} \quad [43]$$

This ensures that the hard pulse will correctly refocus the magnetization.

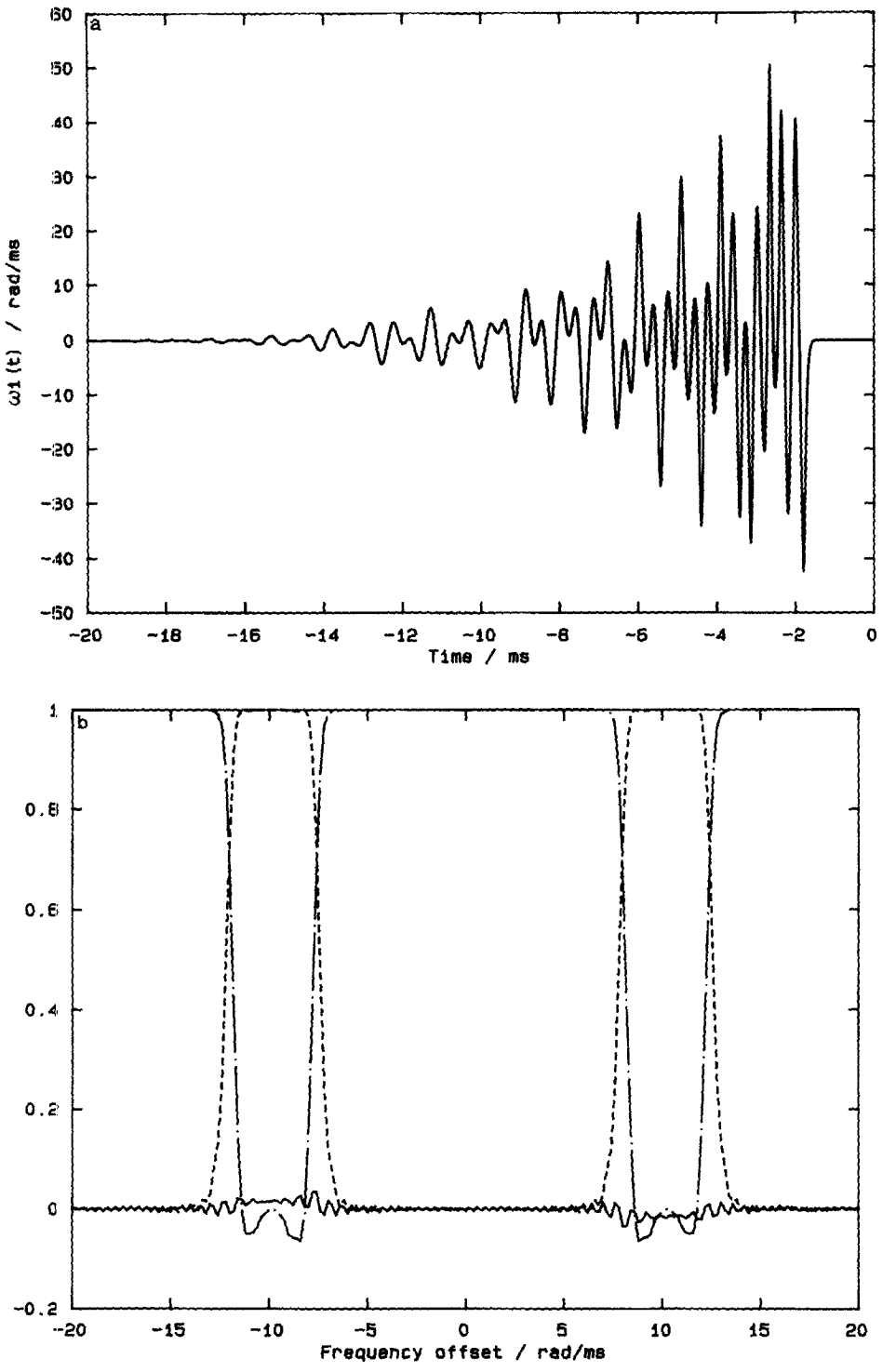

FIG. 5. (a) The pulse envelope and (b) the response to this pulse, obtained from the IST of a rational approximation to a 90° doubly selective pulse, with $n = 7$ (defined in Eq. [40]).

The pulse envelope is shown in Fig. 6 together with the corresponding magnetization responses (for clarity, the m_3 response is not shown). We have chosen the pulse so that it has approximately the same duration as the pulse in Fig. 5 (which we will refer to as the "IST pulse") and so that the two target magnetizations are the same.

We note that the modulated sinc has an amplitude considerably smaller than that of the IST pulse (by a factor of approximately 25). It must be remembered, however, that the IST pulse is self-refocusing, whereas the sinc pulse requires a refocusing hard 180° pulse, which has the possibly undesirable effect of inverting all the spins that are out of the selected slices. Possibly more important is that the IST pulse is an exact inversion of the Bloch equation, and hence the response can be made as good as is required. The sinc pulse, however, is based on a first-order approximation of the system; hence the response may not be sufficiently good. Subsequent numerical optimization of this pulse may improve the response slightly. However, it is often found that optimization improves one feature of the response at the expense of others.

EXAMPLE 4

We have noted in the previous example that self-refocusing pulses require considerably more amplitude than pulses that are refocused with a gradient reversal or 180° hard pulse. These latter pulses are always obtained via Fourier analysis (followed possibly by numerical optimization). We shall now use the IST in order to design an arbitrarily good nonrefocused pulse. We shall find that the resultant pulse is very similar to that obtained via Fourier analysis, and hence it will possess its qualities of small amplitude and favorable behavior with regard to B_1 inhomogeneity.

We shall design a 90° selective pulse of duration τ_0 that requires a refocusing period of duration $\tau_0/2$ before the final magnetization is of the form (defined for ξ real)

$$m_1 = 0 \qquad \text{for all } \xi.$$

$$m_2 = \begin{cases} 0 & \text{for } |\xi| > L/2 \\ 1 & \text{for } |\xi| \leq L/2 \end{cases}$$

$$m_3 = \begin{cases} 1 & \text{for } |\xi| > L/2 \\ 0 & \text{for } |\xi| \leq L/2, \end{cases} \qquad [44]$$

where $L/2$ is the half-width of the excitation.

Suppose that the pulse is defined from $-\tau_0/2 \leq \tau < \tau_0/2$. Then we must have at $\tau = \tau_0/2$ (just before the refocusing starts)

$$\begin{aligned} m &= ie^{i\xi\tau_0} \\ m_3 &= 0 \end{aligned} \qquad \text{inside the slice}$$

and

$$\begin{aligned} m &= 0 \\ m_3 &= 1 \end{aligned} \qquad \text{outside the slice.}$$

This is therefore the magnetization that we want to achieve. We determine the corresponding reflection coefficient by considering how m varies for $\tau > \tau_0/2$ *if no refocusing were applied.* Then inside the slice,

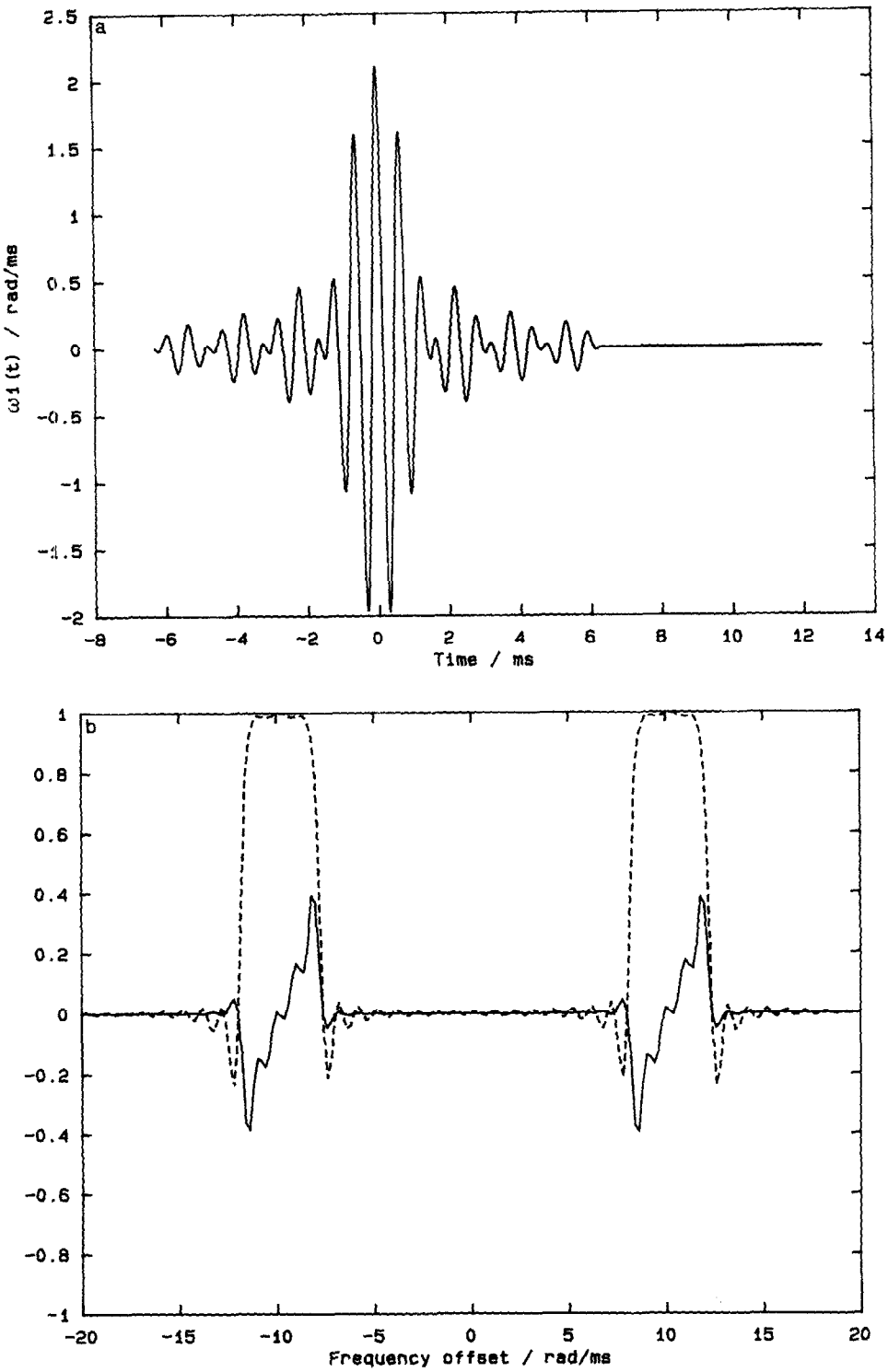

FIG. 6. (a) Modulated sinc pulse designed by Fourier analysis to give an approximately doubly selective pulse. (b) The corresponding m_x and m_y magnetization responses.

$$m(\tau > \tau_0/2) = ie^{i\xi\tau_0}e^{2i\xi(\tau-\tau_0/2)} = ie^{2i\xi\tau}$$

and $m = 0$ outside. Therefore, using Eq. [15],

$$r(\xi) = \begin{cases} 0 & \text{for } |\xi| > L/2 \\ i & \text{for } |\xi| \leqslant L/2 \end{cases} \qquad \text{with } \xi \text{ real.} \qquad [45]$$

We shall now assume that $r(\xi)$ has no poles in the upper half-plane. Then, as shown in Eq. [23],

$$\begin{aligned} f(\tau) &= \frac{1}{2\pi}\int_{-\infty}^{\infty} r(k)e^{ik\tau}dk \\ &= \frac{i}{2\pi}\int_{-L/2}^{L/2} e^{ik\tau}dk \\ &= \frac{iL}{2\pi}\,\mathrm{sinc}(L\tau/2). \end{aligned} \qquad [46]$$

We now use Eq. [21] to get a first approximation to the required pulse envelope, $\omega_0(t)$. Recall [21] that

$$\mathbf{K}_0(\tau, \tau') = -\mathbf{F}(\tau + \tau');$$

hence from Eqs. [10] and [20],

$$\omega_0(t) = -\frac{2L}{\pi T}\,\mathrm{sinc}(Lt/T), \qquad [47]$$

which is simply a sinc envelope, as obtained in Fourier analysis. We can now use the iterative procedure [22] to generate successively better pulse envelopes.

As might be expected, the sharpness of the desired transition region causes a Gibbs phenomenon. Hence it is advisable to multiply $f(\tau)$ by a "windowing" function, so that the transition region has a finite width. For simplicity, we choose a Gaussian window, so that

$$f(\tau) = \frac{iL}{2\pi}\,\mathrm{sinc}(L\tau/2)e^{-\beta\tau^2}, \qquad [48]$$

where increasing β will increase the width of the transition region.

Setting $L = 5$ and $\beta = [L/(4\pi)]^2\log_e 1.2$, we iterated [22] to obtain a pulse envelope $\omega_{\mathrm{opt}}(t)$. We iterated at each time step until the algorithm considered that convergence had been reached. For many time steps, this only took in the region of five iterations. The pulses $\omega_0(t)$ and $\omega_{\mathrm{opt}}(t)$ are shown in Fig. 7. The pulses are shown from $t = -10$ ms to $t = 10$ ms. These pulses need to be followed by a gradient-reversal or 180° hard pulse, and subsequent refocusing for 10 ms. We simulated both pulses and show the corresponding magnetization profiles in Fig. 8.

We see that the response has improved dramatically. Any deviation from a completely perfect response is probably due to rounding errors in the algorithm. It is important to note that this procedure is *not* a numerical optimization—the iterations converge to the correct pulse shape and are not troubled by local minima in the error function.

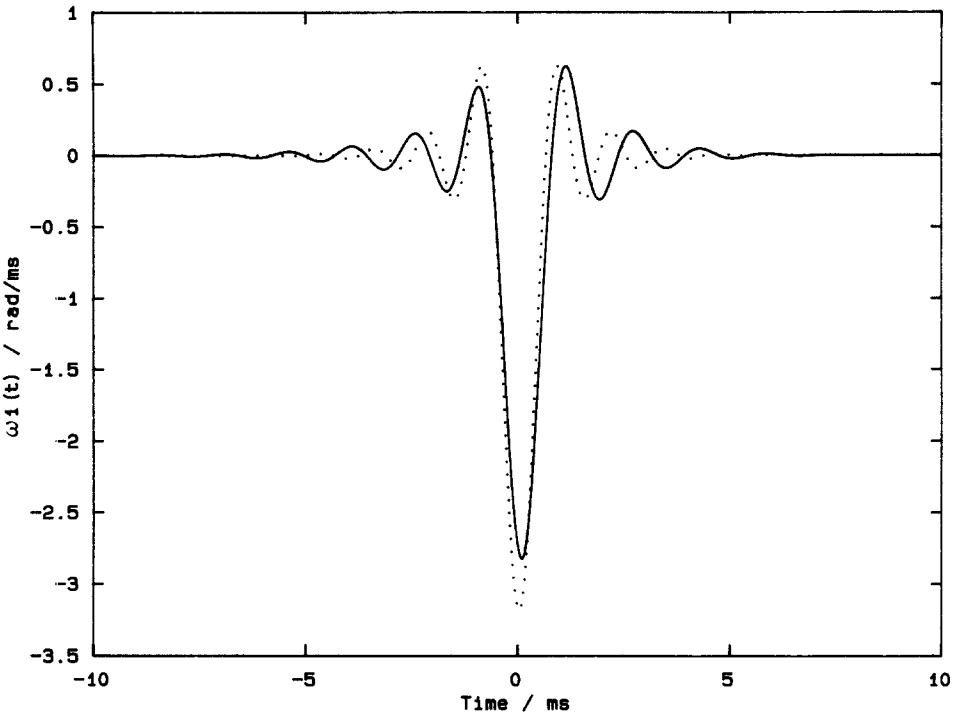

FIG. 7. The pulse envelopes for a 90° selective pulse, needing refocusing. The dotted line is the first-order pulse $\omega_0(t)$. The solid line is the pulse after iterations of Eq. [22], $\omega_{opt}(t)$.

The selective 90° pulses in this example and in example 2 required the same reflection coefficient (at least when defined over real ξ), despite the fact that the resultant pulses were different. This does not violate the result stated earlier that the IST gives a unique solution for a given reflection coefficient, since these reflection coefficients are different when considered over the whole complex plane.

In general, we can design a pulse by assuming that it produces the required magnetization profile at $\tau = 0$. We then determine the reflection coefficient $r(\xi)$ from Eq. [15], which from our assumption above gives

$$r(\xi) = \frac{m(\xi)}{1 + m_3(\xi)}. \qquad [49]$$

If we now use the rational polynomial method, the resultant pulse will indeed produce the desired magnetization profile at $\tau = 0$. The iterative method, however, produces a pulse that does not become zero after $\tau = 0$. The pulse, however will become *negligible* after some time, say $\tau = \tau_{negl}$, and we find that a refocusing period from $\tau_{negl} < \tau \leqslant 2\tau_{negl}$ will result in the magnetization being as required.

B_1 INHOMOGENEITY

We find that the pulses in examples 2 and 3 are sensitive to B_1 inhomogeneity. However, they have been obtained using an analytic one-to-one inversion. Therefore,

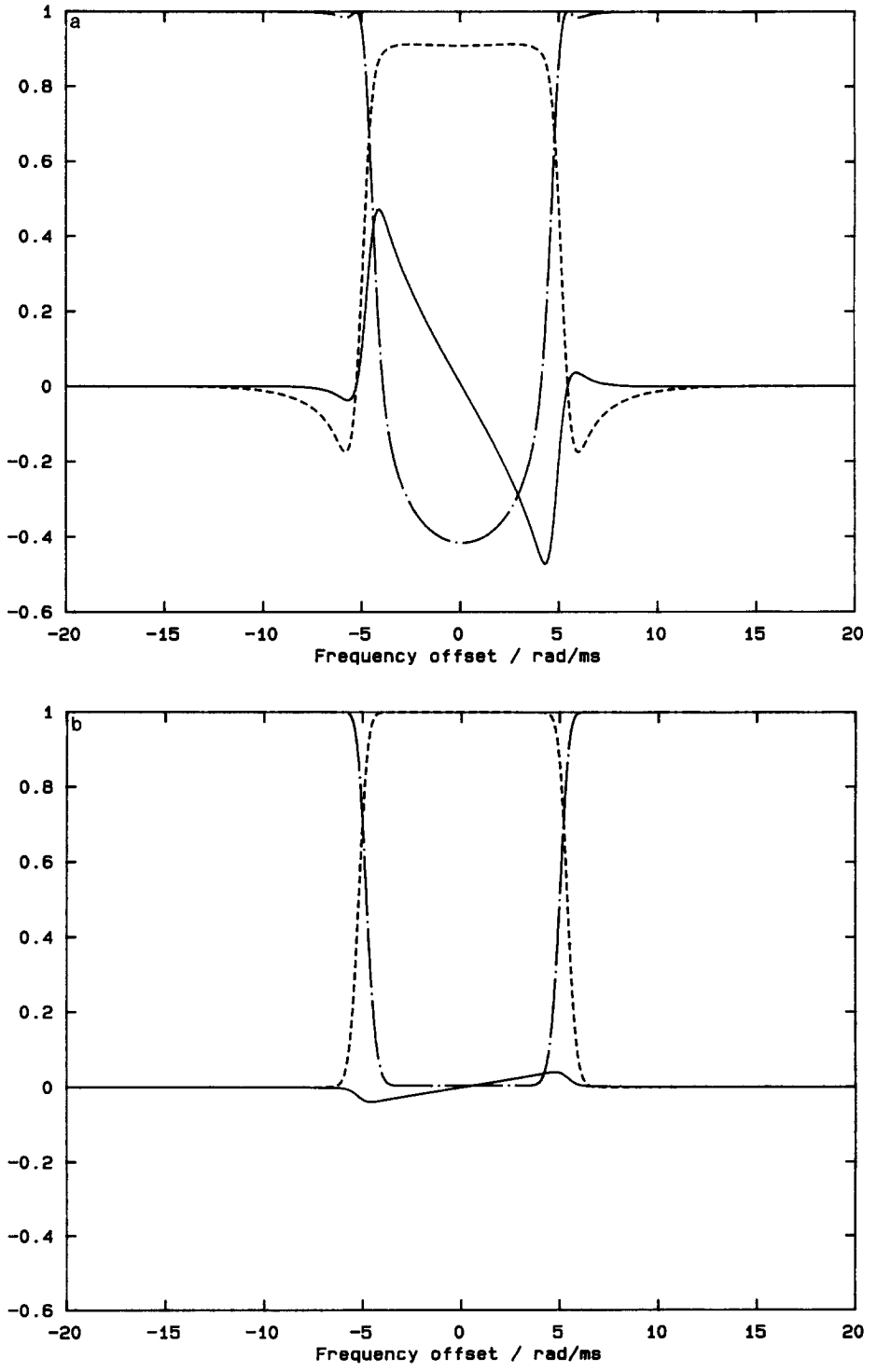

FIG. 8. (a) The response to the pulse $\omega_0(t)$ shown in Fig. 7. (b) The response to the pulse $\omega_{opt}(t)$ shown in Fig. 7.

we expect that the limiting forms of the above pulses (as μ and n tend to ∞) are the only pulse shapes that will yield perfect responses, and so insensitivity to B_1 homogeneity can occur only if we do not insist on such good responses.

Insensitivity to B_1 homogeneity is a feature of frequency-modulated pulses, which is equivalent to the pulse being complex. However, if we require a symmetric magnetization response [corresponding to requiring that $r(\xi) = -r^*(-\xi^*)$], then we have noted that the corresponding pulse must be real. Hence such "adiabatic" pulses seem to be possible only if we choose an asymmetric response.

We remark that the well-known complex hyperbolic secant pulse (*11*) does not give a symmetric response in m_1 and m_2, although the m_3 response is symmetric. Since only the m_3 response is of concern in this case, this pulse is allowed to be complex.

In contrast to examples 2 and 3, the pulse $\omega_{opt}(t)$ obtained in example 4 behaves more satisfactorily with regard to B_1 inhomogeneity. Although the flip angle of the magnetization will be affected, the overall shape of the profile is very stable. Figure 9 shows the magnetization response when the applied pulse has only 50% of the correct amplitude. Together with the fact that the amplitude of $\omega_{opt}(t)$ is only $\frac{1}{16}$ of that of the 20-pole pulse in example 2 and $\frac{1}{70}$ of that of the 84-pole pulse, this suggests that this is preferable provided an additional refocusing gradient or 180° hard pulse is acceptable.

CONCLUSION

We have developed a general method for designing frequency-selective pulses. Given the desired response profiles, it is straightforward to obtain an arbitrarily good rational

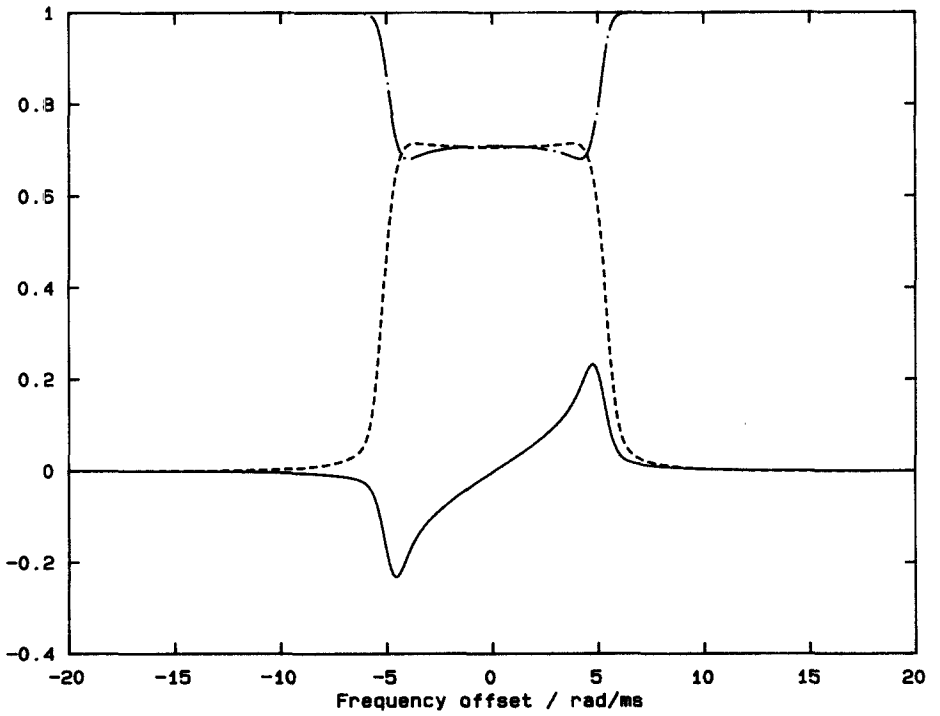

FIG. 9. The response to the pulse $\omega_{opt}(t)$ in Fig. 7, but with only 50% of its amplitude.

approximation to the reflection coefficient and hence apply the inverse scattering transform. We have applied this method to obtain two novel self-refocusing pulse shapes.

Alternatively, we have demonstrated an iterative procedure that is suitable for designing pulses that need refocusing with a hard 180° pulse or a gradient reversal. This procedure is *not* a numerical optimization and hence is untroubled by local minima in the error function.

We have proved an important symmetry result, that a magnetization symmetry of Eq. [25] can occur only if the pulse is real—in conjunction with the well-known converse of this result, we can now state that such a symmetric magnetization response occurs if and only if the pulse is real.

ACKNOWLEDGMENTS

We are grateful to MRC for Grant G8824770 to obtain computing facilities for the design and optimization of selective pulses for MRI and MRS. D.E.R. gratefully acknowledges an SERC case award from Shell Research Ltd.

REFERENCES

1. A. N. GARROWAY, P. K. GRANNELL, AND P. MANSFIELD, *J. Phys. C* **7,** L457 (1974).
2. P. G. MORRIS, "NMR Imaging in Medicine and Biology," Oxford Univ. Press, Oxford, 1986.
3. S. KIRKPATRICK, C. D. GELATT JR., AND M. P. VECCHI, *Science* **220,** 671 (1983).
4. N. METROPOLIS, A. W. ROSENBLUTH, M. N. ROSENBLUTH, A. H. TELLER, AND E. TELLER, *J. Chem. Phys.* **21,** 1087 (1953).
5. P. A. BOTTOMLEY AND C. J. HARDY, *J. Magn. Reson.* **74,** 550 (1987).
6. C. J. HARDY, P. A. BOTTOMLEY, M. O'DONNELL, AND P. ROEMER, *J. Magn. Reson.* **77,** 233 (1988).
7. J. T. NGO AND P. G. MORRIS, *Biochem. Soc. Trans.* **14,** 1271 (1986).
8. J. T. NGO AND P. G. MORRIS, *Magn. Reson. Med.* **5,** 217 (1987).
9. X.-L. WU AND R. FREEMAN, *J. Magn. Reson.* **85,** 414 (1989).
10. J. BAUM, R. TYCKO, AND A. PINES, *J. Chem. Phys.* **79,** 4643 (1983).
11. M. S. SILVER, R. I. JOSEPH, C. N. CHEN, V. J. SANK, AND D. I. HOULT, *Nature* **310,** 681 (1984).
12. I. M. GEL'FAND AND B. M. LEVITAN, *Izv. Akad. Nauk. SSSR Ser. Mat.* **15,** 309 (1951).
13. V. A. MARCHENKO, *Dokl. Akad. Nauk. SSSR* **104,** 695 (1955).
14. I. KAY AND H. E. MOSES, *Nuovo Cim.* **10,** 276 (1956).
15. G. S. GARDNER, J. M. GREENE, M. D. KRUSKAL, AND R. M. MIURA, *Phys. Rev. Lett.* **19,** 1095 (1967).
16. V. E. ZAKHAROV AND A. B. SHABAT, *Sov. Phys. JETP* **34,** 62 (1972).
17. M. J. ABLOWITZ, D. J. KAUP, A. C. NEWELL, AND H. SEGUR, *Stud. Appl. Math.* **53,** 249 (1974).
18. G. L. LAMB, *Phys. Rev. A* **9,** 422 (1974).
19. C. BARRATT, E. D. FACKERELL, AND D. ROSENFELD, *J. Magn. Reson.* **85,** 35 (1989).
20. S. L. ALTMANN, "Rotations, Quaternions and Double Groups," Chap. 11, Oxford Univ. Press, Oxford, 1986.
21. H. E. MOSES AND R. T. PROSSER, *J. Math. Phys.* **25,** 108 (1984).
22. J. T. NGO AND P. G. MORRIS, *J. Magn. Reson.* **74,** 122 (1987).
23. J. FRIEDRICH, S. DAVIES, AND R. FREEMAN, *J. Magn. Reson.* **75,** 390 (1987).